Supporting Information For

Analgesic Microneedle Patch for Neuropathic Pain Therapy

Xi Xie[1,2,+,], Conrado Pascual[1,3,+], Seajin Oh[1], Christopher Lieu[1], Ji Wang[4], Bende Zou[1], Julian Xie[1], Zhaohui Li[1], James Xie[1], David C. Yeomans[3], Mei X. Wu[4], and Xinmin (Simon) Xie[1,3 *]*

[1]AfaSci Research Laboratories, Redwood City, CA, USA

[2]School of Electronics and Information Technology; State Key Laboratory of Optoelectronic Materials and Technologies, Sun Yat-Sen University, Guangzhou, China

[3]Department of Anesthesia, Stanford University School of Medicine, Stanford, CA, USA

[4]Wellman Center for Photomedicine, Massachusetts General Hospital, Department of Dermatology, Harvard Medical School, Boston, MA, USA

S1. Novelty clarification on the Analgesic Microneedles.

Although the concept of microneedles has been put forward for years, to the best of our knowledge, there are only two areas that microneedle delivery has shown real medical promise: using microneedles for vaccination or insulin delivery. Using "pain-free" microneedles to treat pain, especially neuropathic pain, has been a great scientific and medical interest, but few existing reports have shown the unique therapeutic advantages of using microneedles on treating pain, or even any therapeutic evaluation on animals. One important reason for this is that many current medications, such as lidocaine, are essentially anesthetics that nonspecifically block nerve impulses (e.g. benumb tissues), and often require high doses for effective analgesia. These features are not well-suited with microneedles for persistent pain treatment, because dissolvable microneedles have a drug-loading-limitation.

Unlike using microneedles to deliver well-documented clinical drugs, our novelty lies in the creative use of microneedles to test a hypothesis that peripheral blockade of CGRP pathway can effectively treat localized neuropathic pain. Neuropathic pain conditions are not effectively treated by currently available analgesics which often cause either systemic side effects or interfere with normal locomotor function. Our approach, unlike lidocaine, preferentially relieves persistent pain without interfering with normal nociception and motor function. Our approach is also superior to gabapentin, the “gold standard” for treating localized neuropathic pain, because it completely avoids any systemic side effects.

S2. Additional information about CGRP.

The sequence of CGRP is: ACDTATCVTHRLAGLLSRSGGVVKNNFVPTNVGSKAF-NH_2. CGRP, a 37 amino acid peptide, is generated from a specific splicing of calcitonin and mainly synthesized in the somata of nociceptive neurons in the dorsal root ganglion (DRG).[1,2] CGRP can be transported to the peripheral and central nerve endings where it can be released upon intensive activation of those afferents.[3] Nerve or tissue injury, trauma or inflammation triggers release of neuropeptides including CGRP from afferent nerve endings, and in turn CGRP enhances nociceptive neuronal activity.[4] When released from nerve terminals, CGRP binds to a heteromeric receptor of calcitonin receptor-like receptor and receptor activity-modifying protein, and increases nociceptive sensitivity in response to non-noxious mechanical and thermal stimuli under normal conditions. Whereas under pathological conditions, CGRP released in excess prolongs and enhances vasodilatation and plasma extravasation initiated by inflammatory mediators such as histamine, prostaglandins (*e.g.*, PGE2), and cytokines. Thus, excessive CGRP produces thermal hyperalgesia and mechanical allodynia, a condition in which pain is induced by otherwise non-noxious stimuli, and plays a critical role in development of neurogenic inflammatory and chronic pain (Figure S2).[3,5] In preclinical research, using a gene knockout approach, mice lacking CGRP display an attenuated response to chemical-induced pain and inflammation. Using antisense sequence to knock down CGRP specifically in sensory neurons produced a reduction of CGRP levels, and also a decrease in the behavioral hyperalgesia that resulted from capsaicin stimulation.[6]

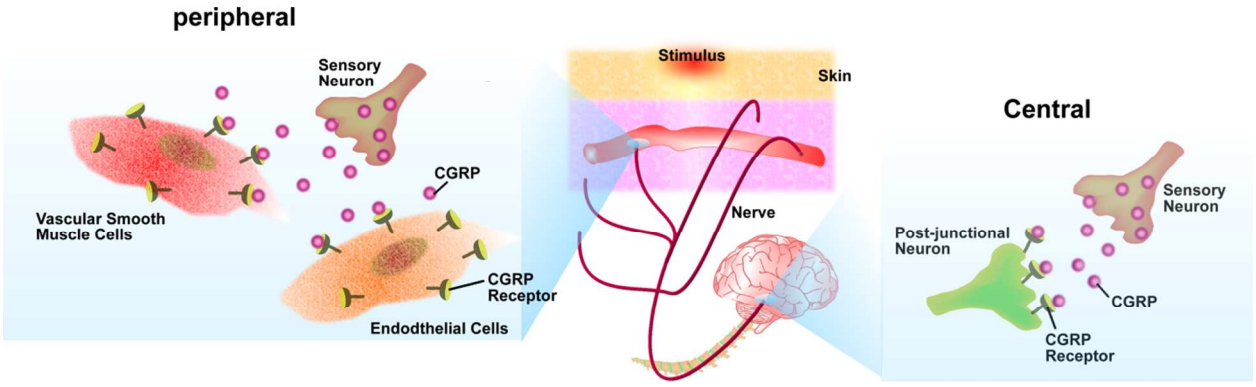

Figure S2. Illustration of the action of CGRP in both peripheral and central nerves. Nervous terminals or tissue injury, trauma or inflammation triggers release of neuropeptides including CGRP from afferent nerve endings, and in turn CGRP enhances nociceptive neuronal

activity. Whereas, excessively released CGRP prolongs and enhances vasodilatation and plasma extravasation initiated by inflammatory mediators.

S3. Supplemental information about CGRP8-37.

The sequence of CGRP8-37: VTHRLAGLLSRSGGVVKDNFVPTNVGSEAF-NH_2. CGRP 8-37 is a 31 amino acid fragment of CGRP that lacks seven N-terminal amino acids. It binds strongly to CGRP receptors without activation.[7] Intravenous injection of a variety of anti-CGRP antibodies and or intrathecal administration of human CGRP 8-37 has been found to significantly attenuate chemical (*e.g.*, capsaicin or acetic acid as well as CGRP)-induced hypersensitivity via blockade of CGRP receptors.[8,9]

Binding assay:[10] both human calcitonin CGRP1 (CGRP1) membrane and [125I]-CGRP were purchased from Perkin Elmer (Waltham, Massachusetts). CGRP1 membrane was homogenized in the assay buffer (50 mM Tris-HCl pH 7.4, 5mM $MgCl_2$, 0.5% BSA, 0.05% Tween20). The CGRP1 membranes were incubated with the test compounds in the presence of 0.24 nM of [125I]-CGRP. After 1 h of incubation, at room temperature, samples were filtered, using a Tomtec cell harvester, through glass fiber filters that had been presoaked in 0.05% polyethyleneimine and washed with the cold Tris buffer (50 mM Tris-HCl pH7.4). Filters were counted on a betaplate reader (Wallac). Nonspecific binding was determined by using 1 μM of rat CGRP peptide. IC_{50} values and hillslope values were determined by using the program Graphpad/PRISM. ki values were calculated using the Cheng Prusoff transformation: $k_i = IC50/(1+L/k_d)$, where, L is radioligand concentration and k_d is the binding affinity of the radioligand, as determined previously by saturation analysis. k_i is the inhibition constant for a peptide, which represents the concentration of competing ligand in a competition assay which would occupy 50% of the receptors (1 μM) if no ligand were present. Table 1 shows the binding affinity of CGRP and representative CGRP antagonist peptides on CGRP receptors under our experimental conditions..

Table 1. Binding affinity of CGRP and CGRP antagonist peptides on CGRP receptors

Compound	Ki (nM)	Hill slope
CGRP	8.9±1.0	0.80±0.07
CGRP 8-37	59.8±0.4	1.21±0.20

Experiments were performed in triplicate and repeated twice. Data are presented as Mean ± SD.

S4-1. Additional notes on different drugs for neuropathic pain treatment.

Medicine	Administration	Results	References
Antiepileptics (e.g., gabapentin, carbamazepine and lamotrigine), Anti-depressants (amitryptiline and duloxetine), Nonsteroidal anti-inflammatory drugs (NSAIDS, e.g., tramadol) Narcotic analgesics (e.g., oxycontin).	Oral	Limited effectiveness; Systematic side effects	[11-18]
Sodium channel blockers (e.g. lidocaine and bupivacaine)	Transdermal Injection	Limited effectiveness; Side effects; Affect normal nociception Unsuitable for self-administration	[19-26]
Non-peptide CGRP antagonist (e.g. BIBN4096 and MK-0974)	Oral	Effective on Migraine; Systematic side effects	[27-32]
Peptide CGRP antagonist (e.g. CGRP8-37)	Oral	Less effective	[32]
	Transdermal Injection	Effective; Fewer side-effects Unsuitable self-administration	[8,9]

S4-2. Comparison of Different Drug Delivery Techniques.

Method of Delivery	Characteristics
Oral	Patient self-administration; Limited by absorption and metabolism; Systematic side effects
Transdermal metal needle injection	Localized; Invasive; painful; Not suitable for self-administration
Microneedle	Painless; Suitable for self-administration; Localized, but larger area than needle injection

S5. Supplemental information for enzyme immunoassay (EIA).

The effective amount of CGRP8-37 in the MN patch was determined with Calcitonin Gene Related Peptide (CGRP) - Enzyme Immunoassay (EIA) Kit (Phoenix Pharmaceuticals, Inc.). This EIA kit has 100% cross-reactivity with CGRP8-37. This enzyme immunoassay kit detects the peptides based on the principle of "competitive" enzyme immunoassay. Briefly, the immunoplate in the kit was pre-coated with a secondary antibody and the nonspecific binding sites of the immunoplate were blocked. The secondary antibody can bind to the F_c fragment of primary peptide antibody whose F_{ab} fragment would be competitively bound by both the targeted peptide and the biotinylated peptide. The biotinylated peptide interacts with streptavidin-horseradish peroxidase (SA-HRP) that catalyzes the substrate solution. The light absorption intensity of the substrate solution is directly proportional to the amount of biotinylated peptide-SA-HRP complex. The binding of the biotinylated peptide is competitive with the samples to the primary peptide antibody. Therefore the light absorption intensity is inversely proportional to the amount of peptide in the samples. The standard curve of the peptide concentration was prepared using the standard peptide provided by the kit. The light absorption intensity was measured using a plate reader (Infinite 200 PRO NanoQuant, Tecan).

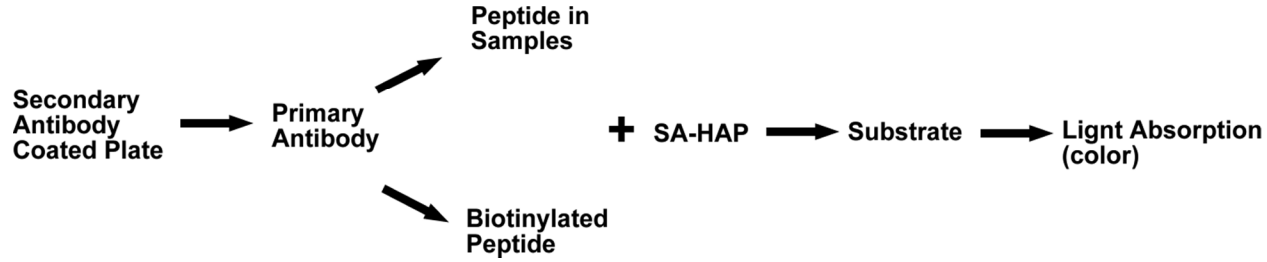

Figure S5. Illustration of the protocol of the EIA.

For the sample in Figure 2f, here are the preparation method and storage conditions:

"Before MN fabrication": 10.0 μg CGRP8-37 was dissolved in 100 μl DI water.

"After MN fabrication": 10.0 μg CGRP8-37 was dissolved in 100 μl 8% SCMC solution, and the solution was poured into the mold and dried overnight to form the MN patch.

"In MNs at 4^{o}C, 1week": the MN samples containing ~10.0 μg CGRP8-37 were stored at 4 ^{o}C for 1 week.

"In MNs, heated to 90^{o}C ": the MN samples containing ~10.0 µg CGRP8-37 were heated up to 90 ^{o}C for 30 min to destabilize the CGRP8-37. This was used as negative control to confirm that the EIA can be used to determine the effective amount of CGRP8-37.

"MNs w/o peptide": the MN was fabricated without loading CGRP8-37. This was used as negative control to confirm that the EIA is specific to CGRP8-37 rather than SCMC.

Each sample was diluted with another 900 µl DI water, and the CGRP8-37 concentration of each solution was measured with the EIA according to the standard protocol of the product.

S6. Supplemental information for MN-mediated fluorescent dye delivery.

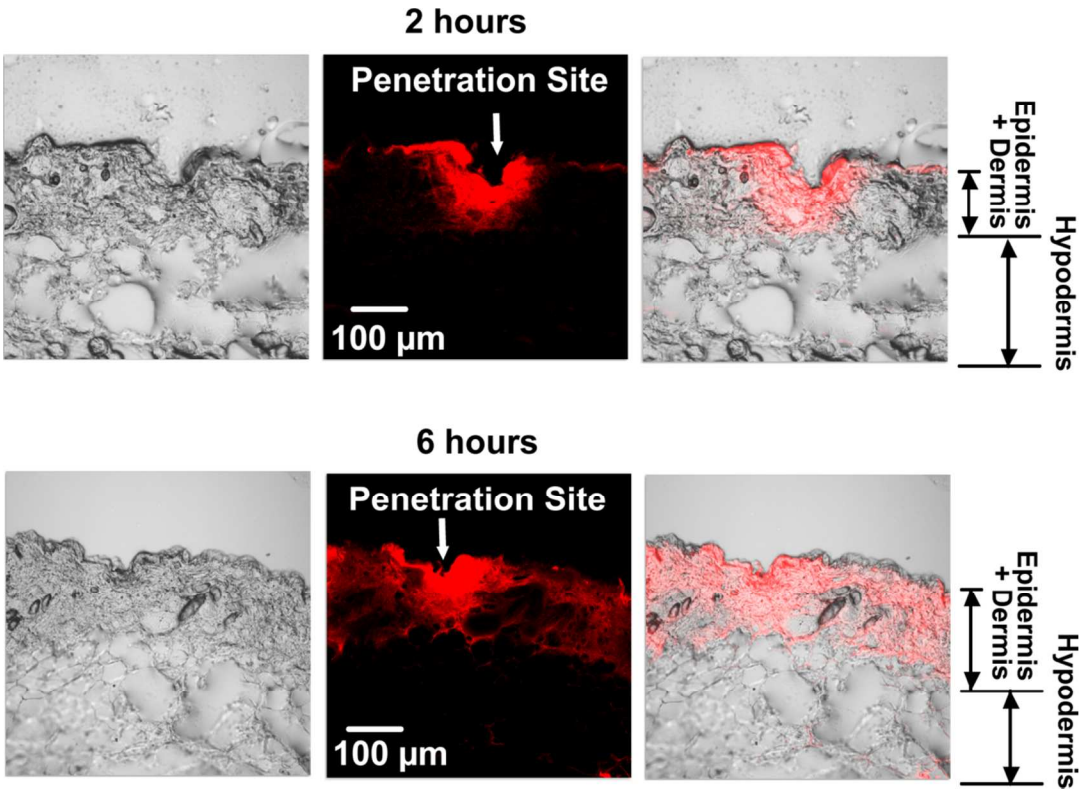

Figure S6-1. From left to right panels, optical images, fluorescence images, and overlap images showing the release of fluorescent molecules from the MNs into rat skins and their spatial distribution.

S6-2. Comparison of fluorescent molecule delivery into skin with microneedles and topical applications.

The stratum corneum (the outermost layer of the epidermis, as illustrated in Figure S6-2a) of skin is a barrier that can prevent many types of drugs from penetrating into the skin tissues. Spontaneous penetration of peptides through the stratum corneum is much more difficult to occur since peptides are larger and charged molecules (REF: *Nature Biotechnology,* 2008, **26**, 1261 - 1268; *Nature Reviews Drug Discovery,* 2004, **3**, 115-124). Previously we observed that topical applications of the anti-CGRP peptide simply in the form of a patch, solution or hydrogel produced no skin penetration and no analgesic effects. In addition, confocal fluorescence studies revealed that the red fluorescent analogue molecule to CGRP8-37, dextran-Rhodamine B (molecular weight ~ 3200; the molecular weight of CGRP8-37 is 3128), cannot penetrate through stratum corneum simply with topical application (Figure S6-2b,c).

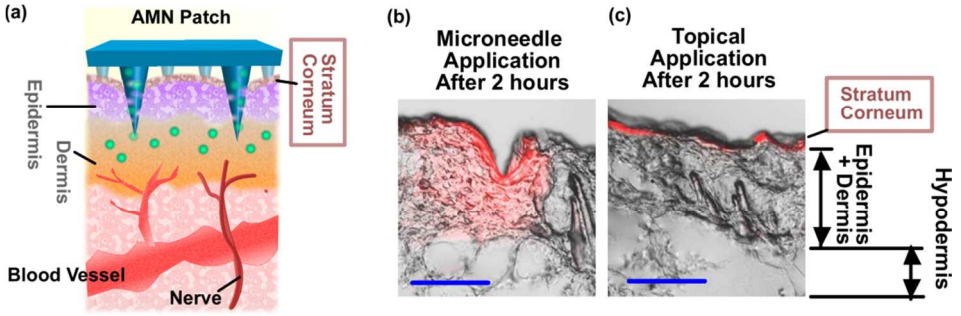

Figure S6-2. (a) Illustration of the Stratum Corneum of skin, which is the outermost layer of the epidermis. Microneedles are used to penetrate only the stratum corneum, but are short enough to not reach the blood capillaries or nerve endings in the dermis layer, so it does not induce pain during application. (b) and (c) Confocal fluorescence microscopy image (red) overlapped with optical image showing the release of red fluorescent molecules (dextran-Rhodamine B, molecular weight ~ 3200; the molecular weight of CGRP8-37 is 3128) into rat skin, either by microneedle application (b), or by topical solution application (c). The skin were dissected 2 h or after MNs insertion and then prepared for imaging. Scale bar: 100 μm in (b) and (c).

S6-3. Drug distribution in microneedles.

The fabrication method of microneedles was illustrated in Figure S6-3 in detail. Drug molecule was dissolved in 8% SCMC solution, and then 50 μl of this solution was added to the MN mold and centrifuged at 4000 rpm for 5 min to drive the solution into the cavities (step#1).

The solution out of the cavities was removed after centrifugation and collected for reuse (step#2). After air-drying overnight (step#3), another 200 µl 8% (w/w) SCMC solution alone was poured on the mold and centrifuged at 4000 rpm for 1 min (step#4). The solution was dried overnight to form a MN patch (step#5) and the patch was peeled off from the mold (step#6).

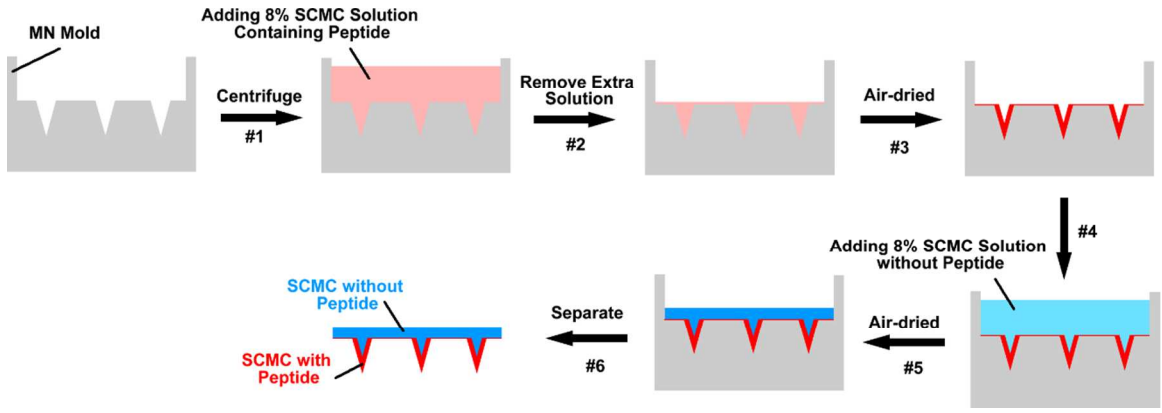

Figure S6-3. Detail illustration of the microneedle patch fabrication.

The drug molecules tend to be loaded in the first 2/3 length of each needle. As shown in the Figure S6-4, the fluorescence-labeled molecules were located in the first 2/3 length of each needle, rather than being located in the whole needle. This can be understood from our illustrated fabrication in Figure S6-3. In step#3, when the 8% CMC solution containing drug molecules was air-dried, the volume of the solution shrank, causing the drug molecules to move closer to the inner sidewall of the microneedle mold. Therefore, the drug molecules were distributed closer to the microneedle tips, allowing effective delivery once the microneedles were inserted into skin.

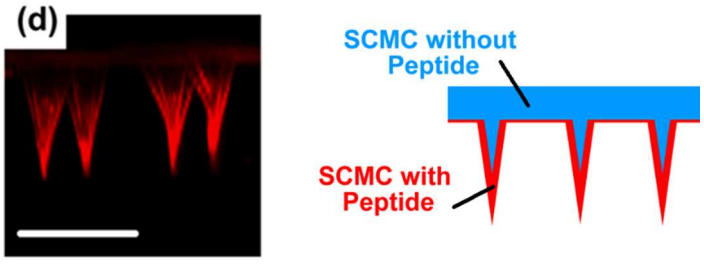

Figure S6-4. Fluorescence-labeled molecules were located in the first 2/3 length of each needle, rather than locating in the whole needle. Scale bar: 1000 µm.

A majority of the peptide drug was transdermally delivered to the local tissue through dissolvable microneedles. When the microneedles were inserted to the skin penetrating the stratum corneum, the microneedle tips were readily dissolved within 20 min. Most of the peptide was immediately released from the dissolved microneedle tips and gradually deposited in the local tissue. This process is illustrated in Figure S6-5.

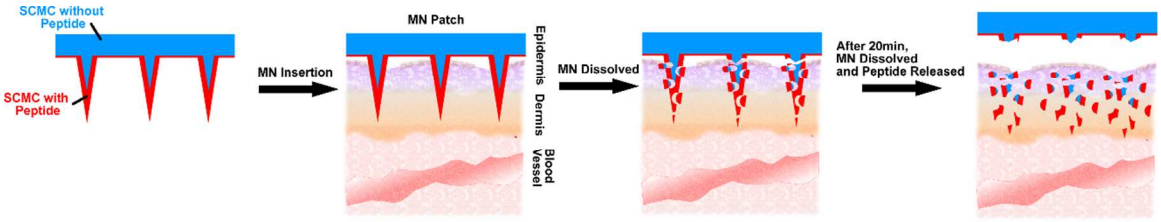

Figure S6-5. Illustration of microneedle insertion and peptide release and deposition into the local tissue.

S7. Discussion on the peptide stability in microneedles in actual applications.

The activity of the encapsulated peptide decreases after storage, but this is not a significant concern. To eliminate the concern of peptide instability, a larger amount of anti-CGRP peptide can be loaded in the microneedle patch to ensure sufficient intact peptides were present for applications. There are two reasons to allow this over-loading. First, the anti-CGRP peptides are safe even at a much higher dose than those we used (as we have demonstrated in Figure 6). The peptides induced very few adverse effects even when we used higher doses of the peptide. Furthermore, most of the microneedles used in this work had been stored for 1 to 4 weeks before use, and they still produced effective analgesia. Although the peptides may lose some activity, it did not significantly affect analgesic performance. For microneedles that require extended periods of storage time, extra peptides can be loaded in the microneedles during fabrication to warrant sufficient intact peptides are present during applications.

S8. Additional information on the dose of lidocaine.

Injection/lidocaine: lidocaine ~750 µg in 50 µl, ~1.5% w/w.

MN/lidocaine: lidocaine ~450 µg/patch; the concentration of lidocaine was determined with light absorption.

Determination of the amount of lidocaine in MNs: MN tips containing lidocaine were immersed in 0.4 ml PBS to allow the tips to be dissolved. Lidocaine has characteristic light absorption at the wavelength of 263 nm. The lidocaine concentration of the solution was

measured with the light absorption at the wavelength of 263 nm using a plate reader (Infinite 200 PRO NanoQuant, Tecan).

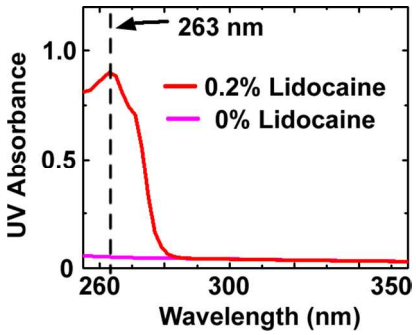

Figure S8. The characteristic light absorption (at wavelength = 263 nm) of lidocaine solution.

S9. Transdermal injection of CGRP8-37 or lidocaine solution to the rat cheek and their potential interference with normal nociception.

In the "UVB/Cheek" model, UVB was administered to the rats' left cheeks to produce an adequate neuroinflammation. The ability of the rats to withstand thermal stimulation was measured by applying noxious heat to the rats' cheeks, and then recording the time it took for the rat to respond to the heat stimuli (withdrawal latencies). 24 hours post-UVB treatment, the rats exhibited hypersensitivity to thermal stimuli ("Before Injection"), compared to that before UVB injuries ("Normal State"). SC injection of CGRP8-37 (1.6 μg in 50 μl) or lidocaine solutions (750 μg in 50 μl, ~1.5%) were administered to the rats' left cheeks. After 20 min, cheek withdrawal latencies in response to noxious heat were assessed at different time points up to 3 hours. As shown in Figure S9a, both CGRP8-37 and lidocaine produced a potent anti-hyperalgesic effect, compared to the hypersensitivity before treatment.

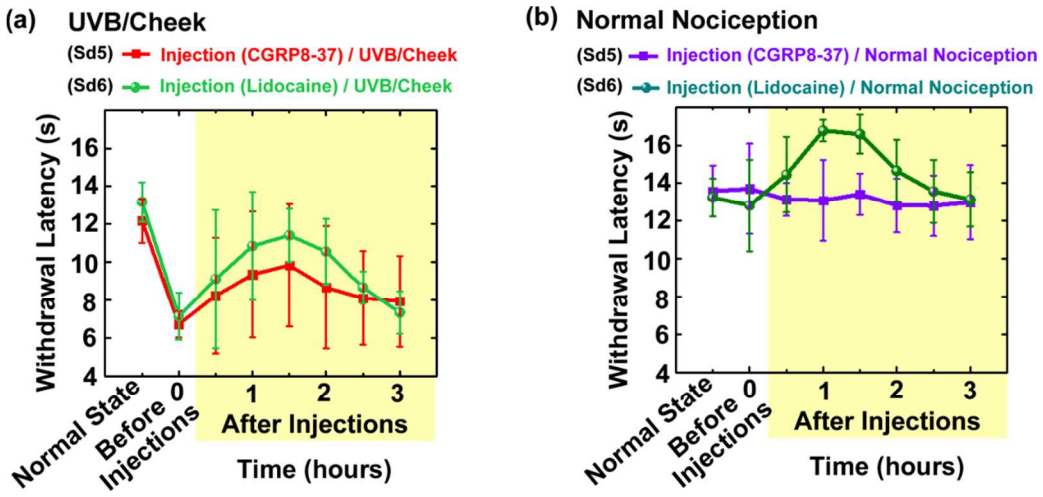

Figure S9. The ability of the rats to withstand thermal stimulation (withdraw latency) was tested for up to 3 h after the treatments with SC injection of CGRP8-37 or lidocaine. These experiments were tested either on (a) "UVB/Cheek" model where the rat cheeks were pre-injured with UVB radiation, or on (b) "Normal Nociception" model where naive rats without any injuries were used.

On the other hand, to test whether SC injection of CGRP8-37 or lidocaine solutions alters normal nociceptive sensation, naive rats without any ongoing inflammation or other pathological pain conditions were used for experiments (Figure S9b). Using similar methods to the cheek pain test but without UVB radiation, the rats' left cheeks were treated with SC injection of CGRP8-37 (1.6 μg in 50 μl) or lidocaine solutions (750 μg in 50 μl, ~1.5%). After 20 min, noxious heat was alternatively applied to both cheeks at different time points, and the cheek withdrawal latencies were measured to assess the rats' nociception. As shown in Figure S9b, the withdrawal latencies of the cheeks treated with Injection/CGRP8-37 showed very little enhancement compared to the pre-injection states, indicating that negligible anesthetic effects on normal nociception were produced by MN/CGRP8-37. In contrast, SC injection of lidocaine (750 μg in 50 μl, ~1.5%), a commonly used clinical dose, produced an anesthetic effect on normal nociceptive pain as expected. The results confirmed that CGRP8-37 injection does not alter normal pain sensation, while lidocaine interferes with normal nociception.

S10. Supplemental information for eating experiments.

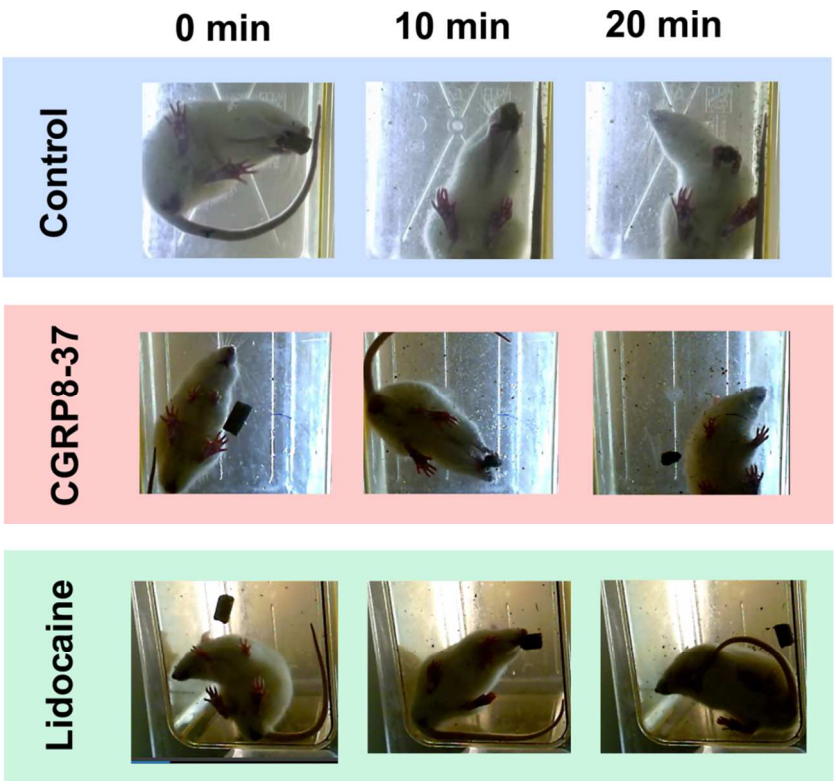

Figure S10. The assessment of local interference with active physical functions after oral mucosa injection of CGRP8-37 or lidocaine. The ability for food-deprived rats to eat one normal rodent food biscuit after injection was tested. The eating process of each group was recorded by a video camera. The rats injected with lidocaine displayed dysfunction of chewing and eating presumably due to local anesthesia as lidocaine blocking both sensory and motor nerve conductivity. The rats injected with CGRP8-37 could eat normally.

S11. Supplemental information for neurobehavioral toxicity experiment.

SC injection of CGRP8-37 solution: ~1.6 μg in 50 μl, ~10 μM. After injection, the CGRP8-37 diffused and spread over a larger area within the skin. Therefore the concentration in the local transdermal space should be much less than the 10 μM of the injected solution. For MN delivery, the amount of CGRP8-37 delivered was ~1.4 μg, and its local concentration in the skin should be much less than 10 μM as well.

The approximate blood volume of a mouse is 77-80 μl/g. For a 25 g mouse this is equivalent to 1.9-2.0 ml. Around 50% blood is plasma, and thus the volume of blood plasma is

~1 ml. 300 μg CGRP8-37 was intravenously injected to the mice every day for 3 consecutive days. The molecular weight of CGRP8-37 is 3128. Therefore the concentration of CGRP8-37 in the blood plasma is ~100 μM. This concentration is much higher than the CGRP8-37 solution used for SC injection (~10 μM), and should be much higher than the local concentration of CGRP8-37 in the skin after transdermal injection or microneedle patch application. However, there were no apparent effects on neurobehavior.

S12. Actual clinical application aspect of the Analgesic Microneedles.

In the future when this technique is further developed to be employed clinically, one potential solution to prolong duration of analgesia is applying the microneedle patch daily to the same pain area once or twice per day. It seems that skin irritation with frequent microneedle application is not a serious concern. For example, there are commercially available microneedle patches containing hyaluronic acid for cosmetic application, and this microneedle product can be used more than once a day (Kim *et al*., International Journal of Cosmetic Science, 2014, 36, 207–212). The commercial product is also available online:

http://www.ebay.com/itm/Spa-Treatment-i-Micro-Patch-2-sheets-4-set-Containing-hyaluronic-acid-Japan-/261792837246?hash=item3cf411ae7e:g:0RAAAOSwZjJU7rkG

In addition to a skin irritation test in which microneedles were applied once a day for 3 consecutive days, we repeated the same test but applied microneedles twice per day for 3 consecutive days attempting to produce acute adverse effects to the skin. On the fourth day, skin samples surrounding the penetration sites were dissected for histology examination. There is little overt infiltrated inflammatory cells in the skin after repeat insertion of MN/CGRP8-37 (Figure S12-1).

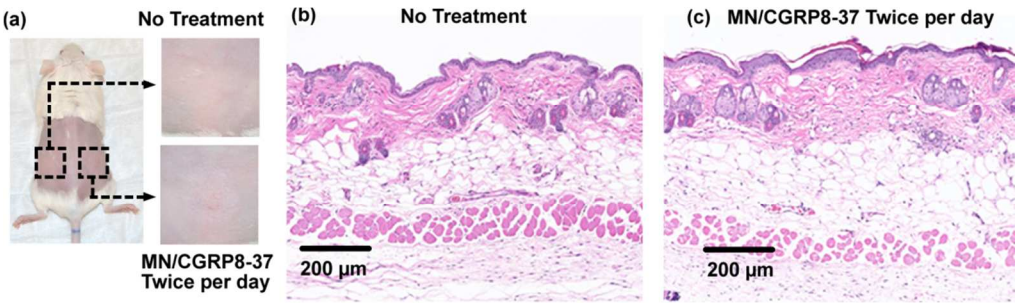

Figure S12-1. (a)-(c) MN/CGRP8-37 (i.e. AMN) treatment did not induce overt skin irritation. Mice were treated with MN/CGRP8-37 twice per day for 3 days. (a) Images were taken on the fourth day. (b) and (c) skin sections were stained by Hematoxylin and eosin (H&E) staining. Each image represents four similar results.

This information indicates that frequent microneedle application on the same skin location is acceptable. For future clinical application, to enhance the peptide's stability and acting duration, the peptide can be optimized by cyclization or pegylation with well-established techniques during peptide synthesis and by formulating the peptide with special encapsulation techniques, for example, mirco- or nano-particles to control the release of peptide from the microneedles. These micro/nano-particles can be further embedded in the microneedles (Figure S12-2). The micro/nano-particles can allow the peptide to maintain higher stability and increase acting duration. In summary, for future clinical application, one needs to optimize the design and the application methods for our current analgesic microneedle patch. A straightforward solution could be the combination of microneedle and nanoparticle technologies.

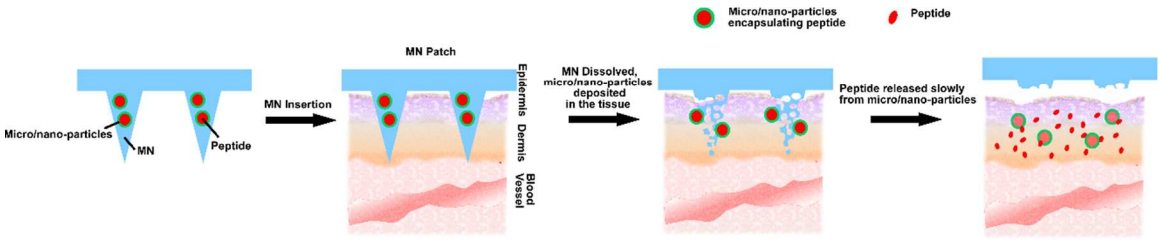

Figure S12-2. Schematic of micro/nano-particles containing peptide and the micro/nano-particles were embedded in microneedles. The peptide can be slowly released from the micro/nano-particles.

S13. Tolerance test of CGRP antagonist peptide.

Compared with chemical drugs, peptide drugs generally have fewer side-effects and little drug tolerance, while the specificity is high. For example, there is little evidence that diabetic patients develop tolerance to daily administration of insulin, nor is there tolerance for patients receiving long-term treatment of pituitary gigantism with octreotide, an octapeptide that mimics natural somatostatin (Otsuka *et al*., Endocr J. 2004 Oct; 51(5):449-52.).

Furthermore, we performed repeated injection of CGRP antagonist peptide daily for 7 consecutive days. Baseline thermal thresholds of rats (Sprague-Dawley, male, 300g - 350g, n=8 per group) were taken prior to surgery. Each rat underwent spared nerve injury (SNI) on its left hind leg. Three weeks post-surgery, the thermal thresholds of each rat was reassessed; presence of hyperalgesia in each rat was confirmed. Eight rats were randomly assigned to receive daily local transdermal injection of CGRP antagonist peptide (~1.6 µg in 50 µl) in the left hindpaw for 7 consecutive days; the remaining 8 rats received a local injection of vehicle as a control. Thermal thresholds were measured each day both prior to local injection and at 2-hour post-injection. As shown in Figure S13, after receiving CGRP antagonist peptide, the rat's thermal threshold increased, indicating successful analgesia. These analgesic effects were reproducible over 7 days. This result indicates that the rat did not develop tolerance on the CGRP antagonist peptide.

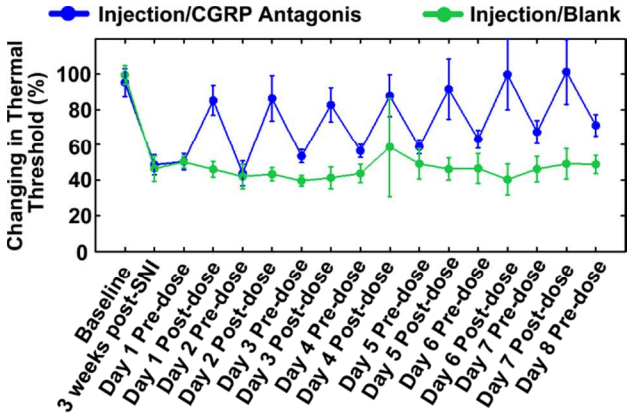

Figure S13. Reproducible analgesic effects following repeated injections of the CGRP antagonist peptide to rats with neuropathic pain daily for 7 consecutive days. Each rat underwent spared nerve injury (SNI) on its left hind leg. Each rat received a daily local transdermal injection of CGRP antagonist peptide (~1.6 µg in 50 µl) or vehicle in the left hindpaw for 7

consecutive days. Thermal thresholds were measured each day both prior to local injection and at 2-hours post-local injection. N=8/group.

Author Information

†These authors contributed equally to this work.

*To whom correspondence may be addressed. Corresponding to: Xi Xie, xiexi27@mail.sysu.edu.cn; or Xinmin (Simon) Xie, simonxie@afasci.com

Reference:

(1) Watkins, H. a; Rathbone, D. L.; Barwell, J.; Hay, D. L.; Poyner, D. R. Structure-Activity Relationships for A-Calcitonin Gene-Related Peptide. *Br. J. Pharmacol.* **2013**, *170*, 1308–1322.

(2) Susan G. Amara, Vivian Jonas, Michael G. Rosenfeld, Estelita S. Ong, R. M. E. Alternative RNA Processing in Calcitonin Gene Expression Generates mRNAs Encoding Different Polypeptide Products. *Nature* **1982**, *298*, 240–244.

(3) Benemei, S.; Nicoletti, P.; Capone, J. G.; Geppetti, P. CGRP Receptors in the Control of Pain and Inflammation. *Curr. Opin. Pharmacol.* **2009**, *9*, 9–14.

(4) Cady, R. J.; Glenn, J. R.; Smith, K. M.; Durham, P. L. Calcitonin Gene-Related Peptide Promotes Cellular Changes in Trigeminal Neurons and Glia Implicated in Peripheral and Central Sensitization. *Mol. Pain* **2011**, *7*, 94.

(5) Jang, J. H.; Nam, T. S.; Paik, K. S.; Leem, J. W. Involvement of Peripherally Released Substance P and Calcitonin Gene-Related Peptide in Mediating Mechanical Hyperalgesia in a Traumatic Neuropathy Model of the Rat. *Neurosci. Lett.* **2004**, *360*, 129–132.

(6) Tzabazis, A. Z.; Pirc, G.; Votta-Velis, E.; Wilson, S. P.; Laurito, C. E.; Yeomans, D. C. Antihyperalgesic Effect of a Recombinant Herpes Virus Encoding Antisense for Calcitonin Gene-Related Peptide. *Anesthesiology* **2007**, *106*, 1196–1203.

(7) Plourde, V.; St-Pierre, S.; Quirion, R. Calcitonin Gene-Related Peptide in Viscerosensitive Response to Colorectal Distension in Rats. *Am J Physiol* **1997**, *273*, G191–G196.

(8) Yu, L.; Hansson, P.; Lundeberg, T. The Calcitonin Gene-Related Peptide Antagonist CGRPs _ 37 Increases the Latency to Withdrawal Responses in Rats. **1994**, *653*, 223–230.

(9) Yu, L. C.; Hansson, P.; Brodda-Jansen, G.; Theodorsson, E.; Lundeberg, T. Intrathecal CGRP8-37-Induced Bilateral Increase in Hindpaw Withdrawal Latency in Rats with Unilateral Inflammation. *Br. J. Pharmacol.* **1996**, *117*, 43–50.

(10) Cheng, Y.; Prusoff, W. H. Relationship between the Inhibition Constant (K1) and the Concentration of Inhibitor Which Causes 50 per Cent Inhibition (I50) of an Enzymatic Reaction. *Biochem. Pharmacol.* **1973**, *22*, 3099–3108.

(11) MacFarlane, B. V; Wright, a; O'Callaghan, J.; Benson, H. a. Chronic Neuropathic Pain and Its Control by Drugs. *Pharmacol. Ther.* **1997**, *75*, 1–19.

(12) Jensen, T. S. Anticonvuls Ants in Neuropa Thic Pain:rationale and Clinical Evidence. *Eur. J. Pain* **2002**, *6*, 61–68.

(13) McQuay, H. J.; Tramér, M.; Nye, B. A.; Carroll, D.; Wiffen, P. J.; Moore, R. A. A Systematic Review of Antidepressants in Neuropathic Pain. *Pain* **1996**, *68*, 217–227.

(14) Saarto, T.; Wiffen, P. J. Antidepressants for Neuropathic Pain (Review). *Cochrane Database Syst. Rev.* **2012**.

(15) Hollingshead, J.; Dühmke, R. M.; Cornblath, D. R. Tramadol for Neuropathic Pain. *Cochrane Database Syst. Rev.* **2006**, *3*, CD003726.

(16) Rowbotham, M. C.; Twilling, L.; Davies, P. S.; Reisner, L.; Taylor, K.; Mohr, D. Oral Opioid Therapy for Chronic Peripheral and Central Neuropathic Pain. *N. Engl. J. Med.* **2003**, *348*, 1223–1232.

(17) Zenz, M.; Strumpf, M.; Tryba, M. Long-Term Oral Opioid Therapy in Patients with Chronic Nonmalignant Pain. *J. Pain Symptom Manage.* **1992**, *7*, 69–77.

(18) Arnér, S.; Meyerson, B. a. Lack of Analgesic Effect of Opioids on Neuropathic and Idiopathic Forms of Pain. *Pain* **1988**, *33*, 11–23.

(19) Eija Kalso. Sodium Channel Blockers in Neuropathic Pain. *Curr. Pharm. Des.* **2005**, *11*, 3005–3011.

(20) Brose, W. G.; Cousins, M. J. Subcutaneous Lidocaine for Treatment of Neuropathic Cancer Pain. *Pain* **1991**, *45*, 145–148.

(21) Yuan, J. S.; Ansari, M.; Samaan, M.; Acosta, E. J. Linker-Based Lecithin Microemulsions for Transdermal Delivery of Lidocaine. *Int. J. Pharm.* **2008**, *349*, 130–143.

(22) Taddio, a; Ohlsson, a; Einarson, T. R.; Stevens, B.; Koren, G. A Systematic Review of Lidocaine-Prilocaine Cream (EMLA) in the Treatment of Acute Pain in Neonates. *Pediatrics* **1998**, *101*, E1.

(23) Johnson, M. E. Potential Neurotoxicity of Spinal Anesthesia with Lidocaine. *Mayo Clin. Proc.* **2000**, *75*, 921–932.

(24) Radwan, I. a M.; Saito, S.; Goto, F. The Neurotoxicity of Local Anesthetics on Growing Neurons: A Comparative Study of Lidocaine, Bupivacaine, Mepivacaine, and Ropivacaine. *Anesth. Analg.* **2002**, *94*, 319–324, table of contents.

(25) Ackerman, W. E. Transient Neurologic Toxicity after Subarachnoid Anesthesia with Hyperbaric 5% Lidocaine. *Anesth. Analg.* **1993**, *77*, 1306.

(26) Perez-Castro, R.; Patel, S.; Garavito-Aguilar, Z. V.; Rosenberg, A.; Recio-Pinto, E.; Zhang, J.; Blanck, T. J. J.; Xu, F. Cytotoxicity of Local Anesthetics in Human Neuronal Cells. *Anesth. Analg.* **2009**, *108*, 997–1007.

(27) Doods, H. Development of CGRP Antagonists for the Treatment of Migraine. *Curr. Opin. Investig. Drugs* **2001**, *2*, 1261–1268.

(28) Farinelli, I.; de Filippis, S.; Coloprisco, G.; Missori, S.; Martelletti, P. Future Drugs for Migraine. *Intern. Emerg. Med.* **2009**, *4*, 367–373.

(29) Blanca Marquez de Prado, A. F. R. CGRP Receptor Antagonists: A New Frontier of Anti-Migraine Medications. *Drug Discov Today Ther Strateg.* **2006**, *3*, 593–597.

(30) Doods, H.; Hallermayer, G.; Wu, D.; Entzeroth, M.; Rudolf, K.; Engel, W.; Eberlein, W. Pharmacological Profile of BIBN4096BS, the First Selective Small Molecule CGRP Antagonist. *Br. J. Pharmacol.* **2000**, *129*, 420–423.

(31) Edvinsson, L.; Nilsson, E.; Jansen-Olesen, I. Inhibitory Effect of BIBN4096BS, CGRP(8-37), a CGRP Antibody and an RNA-Spiegelmer on CGRP Induced Vasodilatation in the Perfused and Non-Perfused Rat Middle Cerebral Artery. *Br. J. Pharmacol.* **2007**, *150*, 633–640.

(32) Stewart J. Tepper MD, M. J. S. M. Clinical and Preclinical Rationale for CGRP-Receptor Antagonists in the Treatment of Migraine. *Headache J. Head Face Pain* **2008**, *48*, 1259–1268.